

# Synthesize of the 31<sup>st</sup> March 2006 (Mw 6.1) Silakhor Earthquake (Iran), using Empirical Green's Functions Method

A. Nicknam<sup>1</sup>, R. Abbasnia<sup>2</sup>, Y. Eslamian<sup>3,\*</sup>, M. Bozorgnasab<sup>3,\*</sup>

1. Assistant professor, Dept of Civil Engineering, the Iran University of Science and Technology, Tehran, Iran.
  2. Associated professor, Dept of Civil Engineering, the Iran University of Science and Technology, Tehran, Iran
  3. Ph.D Student, Dept of Civil Engineering, the Iran University of Science and Technology, Tehran, Iran
- \* Email: [Y\\_eslamian@iust.ac.ir](mailto:Y_eslamian@iust.ac.ir), [M\\_bozorgnasab@iust.ac.ir](mailto:M_bozorgnasab@iust.ac.ir)

## Abstract

The main objective of this paper is to simulate the acceleration time histories, during the Silakhor earthquake in Iran on 31 March 2006 (Mw 6.1). The two selected stations are sufficiently far away from the causative fault so as the observed time series have not been influenced by the near source effects such as directivity and fling step. The well known Empirical Green's function method (EGF) is used for modeling the source-path and site. The method and model parameters are discussed and the appropriateness of selected parameter values are shown. The performance of the selected model parameters are validated by comparing the simulated and observed strong motions data. Good agreement between the estimated strong motion time histories, in the form of Peak Ground Accelerations (PGAs) and elastic response spectra confirm the suitability of the model parameters including source, path and site parameters, consequently the efficiency of the method used for synthesizing ground motions. This model can be reliably used in hazard analysis of existing important structures in the Silakhor region.

**Keywords:** Empirical Green's function method, Silakhor earthquake, Simulation, Fault dimensions, Elastic response spectra.

## 1. INTRODUCTION

Traditionally, in probabilistic seismic hazard analysis approaches (PSHA), either peak ground acceleration (PGA) or response spectrum are estimated to be used in design or retrofit procedure of structures. However, none of these two cases provide complete representation of dynamic behavior of ground motion particularly in nonlinear dynamic analysis of structures. Therefore, realistic time histories are preferred to be used for better understanding the seismic behavior of structures thus reducing uncertainties in estimation of standard engineering parameters. In areas in which there is commonly a lack of recorded strong ground motion, such as the region under study, Silakhor (Iran), the prediction of ground motion expected for hypothetical future earthquakes is often performed by employing empirical models. Various types of synthesized strong motions can be used for this purpose. The first successful attempt for theoretical calculation of strong motions was made by Aki (1968). Kinematic source model was used by propagating dislocation over a fault plane in an infinite homogeneous medium. The approach they proposed contains source parameters such as fault length, fault width; rupture velocity, final offset of dislocation and rise time.

The  $\omega^2$  spectrum-based simulation methodology is based on the stochastic point-source simulation approach for crustal earthquakes (Boore, 1983; Atkinson and Boore, 1995; 1997a, 1997b). In Atkinson approach, each sub-fault is treated as a point source, while the whole source acts as a point source in point-source technique pioneered by Boore (1983). Both techniques are omega-square spectrum based.

According to Boore (2003), the total Fourier spectrum of ground motion as a function of seismic moment  $M_0$ , distance  $R$ , and frequency  $f$  can be described as:

$$Y(M, R, f) = E(M_0, f) * P(R, f) * G(f) * I(f) \quad (1.1)$$

where  $E(M_0, f)$  is the source,  $P(R, f)$  is the path, and  $G(f)$  is the site contribution, respectively. The instrument or type of motion is described by  $I(f)$ .

In Atkinson and Bersenev (1998) technique, the high-frequency seismic field near the epicenter of a large earthquake is modelled by subdividing the fault plane into a certain number of sub-elements and summing their contributions, with appropriate time delays, at the observation point. Each element is treated as a point source with a theoretical  $\omega^2$  spectrum.

In hybrid approaches, the seismogram is modeled by either kinematic (composite) or stochastic approach. The threshold frequency is usually about 1Hz (lower frequencies are deterministic, higher ones are stochastic).

In Green's Function-based methods, the fault is divided into relatively few segments which are assumed to represent small earthquakes. The source time function of each sub-event has its spectral shape, corner frequency, seismic moment, etc. Contributions of sub-events are summed in a special way to get proper seismic moment and spectral shape of the source function corresponding to the whole fault. This approach is often used together with the Empirical Green's Function (EGF) method where a small earthquake is taken as the record of the small rupture, but analytic Green's function can be used as well.

This use of small events as Empirical Green's Function was first proposed by Hartzell (1978). He suggested that the records of small magnitude earthquakes occurring near the main shock fault plane could be taken as Empirical Green's functions (EGFs) in simulating the ground motion for the target region. EGFs include complex effects of the dynamical rupture process on the fault as well as heterogeneous structures around the source and an observation site, which are extremely cumbersome to evaluate.

The possible main shock fault plane is divided into a large number of sub-faults and the contributory ground motion of each sub-fault is obtained by convolving the estimated EGF with a prescribed source time function. The number of such sub-faults is determined from the scaling law of Kanamori and Anderson (1975). Each sub-fault is taken to produce the recorded accelerogram of the aftershock or small magnitude event, with a correction factor (Iyengar et al., 2006). Each such accelerogram is delayed at the surface station to account for rupture time and travel time from the various sub-faults that make up the main fault. In the context of the Silakhor earthquake, strong motion data of three aftershocks, recorded at some stations, are available. Here, the approach of Frankel (1995) requiring a single Green's function is adopted. The main shock fault plane, as reported by Mori (2001), is divided into sub-faults of area:

$$A_s = \left(\frac{M_s}{M_m}\right)^{\frac{2}{3}} A_m \quad (1.2)$$

Here  $M_m$  and  $M_s$  are the moment values of the main event and aftershock, respectively.  $A_m$  is the area of the main shock fault plane taken to be rectangular (Lam. et al. 2000).

Following Frankel (1995), the ground acceleration at Station during the main event can be expressed as a sum of  $N$  convolutions to obtain:

$$\ddot{U}(t) = \sum_{i=1}^N C_i \left(\frac{R}{R_i}\right) [S(t) * u(t - t_{si} - t_{ri})] \quad (1.3)$$

Here  $u(t)$  is the recorded acceleration (EGF) corresponding to sub-fault  $i$ .  $C_i$  is the ratio of the stress drop in the  $i$ -th fault to that of the small aftershock event.  $R_i$  is the distance of the  $i$ -th fault to the surface station and  $R$  is the hypocentral distance between the station and the source of the aftershock. The shear-wave travel time  $t_{si}$  from  $i$ -th fault to the station can be computed from the velocity model.

The EGF is further delayed by the rupture time  $t_{ri}$ , found as the ratio of the distance between the  $i$ -th fault and the main shock hypocenter, to rupture velocity. The stress drop ratio  $C_i$  is taken as (Pitarka et al., 2000):

$$C_i = \left[ \frac{(A_m / A_s)}{\sum_{i=1}^N (d_i / d_{\max})^2} \right]^{\frac{1}{2}} \frac{d_i}{d_{\max}} \quad (1.4)$$

where  $d_i$  is the slip on the  $i$ -th fault and  $d_{\max}$  is the maximum slip. The Fourier transform of the source time function  $S(t)$  is of the form (Frankel, 1995):

$$S(f) = \left( \frac{M_m}{\sum_{i=1}^N C_i M_s} \right) \left[ \frac{1 + (f / f_s)^2}{1 + (f / f_m)^2} \right] \quad (1.5)$$

where,  $f_s$  is the corner frequency of the aftershock records. The corner frequency of the main event record is taken as:

$$f_m = f_s / [\sqrt{(M_m / \sum C_i M_s)}] \quad (1.6)$$

We used Kostrov slip function with Healing Phases proposed by Hutchings. The time delay for the step functions' summation is at the digital sampling rate of the EGFs to ensure that high-frequency artifacts are higher than the frequency range of interest. In the frequency domain, EMPSYN employs a ramp function with all the parameters of the Kostrov or Haskell slip functions. Hutchings (1994) showed that the difference in computed seismograms using the ramp to model the shape of the Kostrov slip function was indistinguishable in the frequency range of 0.5 to at least 15.0 Hz.

## 2. TECTONIC SETTING AND SEISMICITY

From seismically active areas point, Iran includes one of the most severe active faults in the world. This activity primarily results from its position as a 1000-km-wide zone of compression between the colliding Eurasian and Arabian continents. However, still a comprehensive re-analysis of the reported instrumental seismicity data for Iran has not been published to date (Vernant et al., 2004).

The active tectonics of Iran are dominated by the convergence of the Arabian and Eurasian plates which according to GPS data, occurs at about  $22 \pm 2$  mm/yr in the direction N13°E (Vernant et al., 2004).

Over 2000 instrumentally recorded earthquakes occurring in the Iran region during the period 1918–2004 that are well constrained by teleseismic arrival times reported to the ISS, ISC and NEIC have been relocated as single events with special attention to focal depth using the EHB methodology (Engdahl et al., 1998).

The Zagros mountains of SW Iran form a linear intra-continental fold-and-thrust belt about 1200 km long, trending NW-SE between the Arabian shield and central Iran, with a width varying between 200 and 300 km. Roughly 50 percent of the convergence rate between the Arabia Plate and the continental crust of central Iran is accommodated in the Zagros by north-south crustal shortening oblique to the strike of the belt over much of its length (Tatar et al., 2002; Vernant et al., 2004).

Folds within the Zagros contain one of the largest global reserves of hydrocarbons (e.g. Beydoun, 1991). Seismic activity is widespread, with many destructive earthquakes (e.g. Talebian and Jackson, 2004).

In general the main trend of the active fault in the Zagros is in NW-SE and the main active faults in the Lorestan Province are shown in the Figure 1.

At 4:47 a.m. on March 31, 2006 an earthquake occurred in the south of Borujerd with several foreshocks, especially on March 30, 2006 with  $M_L=4.6$  and at 23:06 on March 30, 2006 with  $M_L=5.1$ , and also with the aftershock at 5:01 a.m. on March 31, 2006 with  $M_L=4.9$ . According to news reports, 66 fatalities, about 1280 injuries, and damage to 330 villages in the Darb\_e\_Astaneh (Silakhor) region (surrounding Borujerd and Dorud) reported. The occurrence of this earthquake near the main Zagros fault (section of Dorud fault) shows the probability of further activity from this fault (Figure 1). IIEES's report on the previous earthquakes on May 3, 2005 shows that in this same region, a number of earthquakes of which the greatest magnitude was 4.9 occurred on May 3, 2005 and caused one fatality and great panic among people of this region.

The epicenter of the earthquake on March 31, 2006, was reported to be in the south-eastern epicentral region of that of the May 3, 2005 earthquake with a greater magnitude.

The occurrence of eight earthquakes between May 3-5, 2005 in the Borujerd region, 17 consecutive earthquakes with a magnitude of 2.5-4 between November 21- 27, 2004 in the Poldokhtar region and other similar cases all indicate the high seismic activity of this area. It is estimated that, these earthquakes occurred as the result of stresses

generated by the motion of the Arabian plate northward against the Eurasian plate at a rate of 2 to 3 cm/year (about one inch per year). Deformation of the Earth's crust in response to the plate motion takes place in a broad zone that spans the entire width of Iran and extends into Turkmenistan.

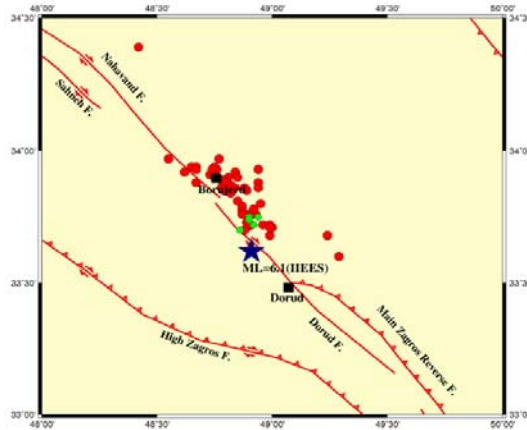


Figure 1 Map of the earthquake's epicenter on 2006 Silakhor ML=6.1 and foreshocks and aftershocks of the earthquake

With regard to the increase in seismic activity of the region, IIEES has dispatched a specialized team to the region on March 31, 2006 with the aim of preliminary identification of the earthquake stricken region and installing a temporary seismic network with 6 seismic stations in the region. More than 60 aftershocks have been recorded by the broad band seismic network of IIEES in the region (Figure 1).

### 3. SOURCE DATA

It is not possible to record empirical Green's functions from all locations along a fault of interest with the same focal mechanism solution. The source locations of empirical Green's functions have been interpolated to fill the sub-fault of fault plain. Interpolation is performed by correcting the attenuation law  $1/R$ , and P, S-wave arrival times due to differences in source distance. We included the radiation pattern effect for low frequencies, when using synthetic Green's functions.

Digitized three-component recordings of aftershocks from the 2006 Silakhor earthquake were obtained by BHRC at stations where strong ground motions caused by the main event were recorded. It is worth mentioning that, the selected stations were sufficiently far away from source (more than 25 kilometers) so that they had not been influenced by near source effects such as directivity and fling step.

Table 3.1 shows the recording site stations, Dorood and Dare-Asbar. The corresponding longitude, orientation and the number of recorded aftershocks are also presented. The site soil conditions, shown in the Table 3.1, are classified according to the Iranian standard No. 2800, which is compatible with those of NEHRP Code.

Table 3.1 Station names, locations and number of EGFs that recorded at each station in 2006 Silakhor Earthquake

Station	Longitude Degree	Latitude Degree	Orient. L,T-90	No of EGF	Geological Classification	
					Standard NO. 2800	NEHRP CODE
Dorood	49.059	33.491	215	2	III-B	D
Dare-Asbar	49.06	33.45	029	2	---	---

#### 4. RESULTS AND DISCUSSION

In order to estimate the strong motions at selected stations, we applied EGF technique which uses the recordings of small earthquakes as empirical Green’s functions. We considered a number of aftershocks in the form of three-components recorded at stations which have been located surrounding the March, 2006 Silakhor main shock Epicenter (BHRC).

The FORTRAN computer program “EMPSYN” originally written by Hutchings (1988) was utilized for synthesizing time histories.

Some investigators reported source parameters of main shock. We changed our model parameters, considering these references, to find good result using EGF method (See table 5.1).

The simulated time series were validated against recorded data at stations sufficiently far away from the causative source with the aim of not being influenced by the near source problems such as directivity and fling step effects. Figure 3 demonstrates the observed and simulated acceleration time histories at Dorood station (L. Component). Also Figures 4 and 5 show the comparison of simulated elastic response spectra at Dorood and Dare-Asbar stations with those of observed data. Good match of synthesized and recorded data confirms the reliability of model used and appropriateness of the selected model parameters. It is notable that, we do not claim that, a) the two well known uncertainties, aleatoric and epistemic, inherently existing in the model parameters are quite minimized and b) the substitution of aftershocks in corresponding sub-faults on the plane source are completely correct, rather, we believe that more research works are required for selecting suitable aftershocks and modifying delay times of the waves radiated from sub-faults to the desired stations.

Table 4.1 Source Parameters of 2006 Silakhor Earthquake proposed and Used in this study

Epicenter			Main Event		Reference
Longitude	Latitude	Depth	Moment	Focal mechanism	
Degree	Degree	( Km)	MW,ML,Mn	(Strike, Dip, Rake)	
44.09	33.69	5.0	6.1 (ML)	-----	BHRC
48.864	33.483	18.0	5.9 (Mn)	-----	IGTU
48.800	33.583	10	5.7 (Mn)	314 , 54 , 180	NEIC
48.78	33.69	12	6.1 (ML)	311 , 54 , -172	CMT
48.91	30.76	14.1	6.1 (ML)	307 , 67 , -148	IEES
---	---	---	6.1 (ML)	315 , 61 , -164	Hamzeloo et al
48.81	33.69	18	6.1(ML)	306 , 63 , -176	Used here

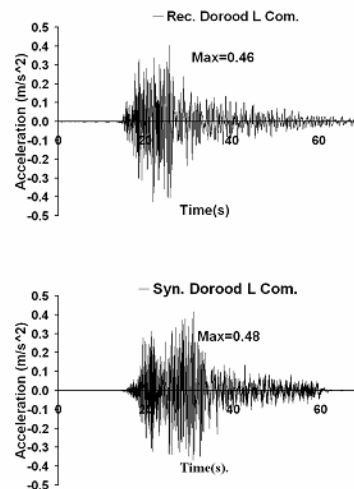


Figure 3 Comparison of synthesized Acceleration time history at Dorood St. with those of the recorded data

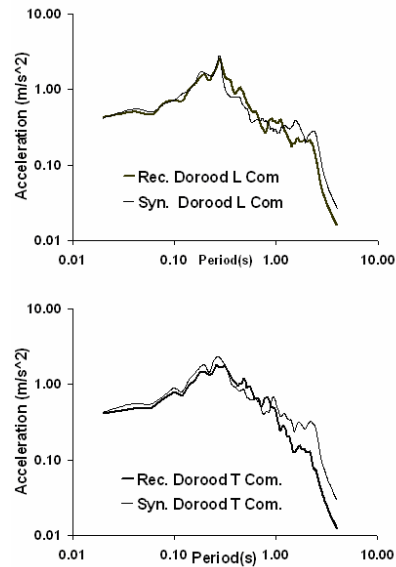


Figure 4 Comparison of synthesized elastic response spectra at Dorood Station with those of the recorded data

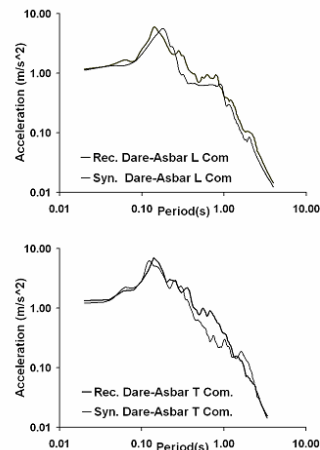


Figure 5 Comparison of synthesized elastic response spectra at Dare-Asbar St. with those of the recorded data

## 5. CONCLUSION

We simulated the recorded strong motions at selected stations using the well known EGF approach and utilizing the FORTRAN computer program EMPSYN originally written by Hutchings. The selected stations were far away from the causative fault so that it can be evaluated as a far field event rather than near field. The synthesized strong motions are validated against the observed data in the form of elastic response spectra. Rather good agreement of these two plots shows the reliability of the synthesizing far field strong motions procedure, including the selected model parameters such as fault dimensions, slip function and hypocenter location.

The model used in this study can be utilized in hazard analysis of important structures and also in retrofitting procedure of historical buildings in the region under study.

## 6. ACKNOWLEDGMENTS

Many thanks to Professor Hutchings for kindly offering the valuable simulation codes and Dr. Yasin Fahjan for giving windows EMPSYN FORTRAN Codes.

## REFERENCES

- Aki, K., (1968). Seismic displacements near a fault. *J. Geophys. Res.* 73(6), 5359-5376.
- Atkinson, G.M., Boore, D. M., Ground-motion relations for eastern North America. (1995). *Bull. Seism. Soc. Am.* 85, 17-30.
- Atkinson G.M., Boore, D.B., (1997a). Source comparisons between recent ground motion relations. *Seism. Res. Lett.* 68, 24-40.
- Atkinson, G.M., Boore, D.B., (1997b). Stochastic point source modelling of ground motions in the Cascadia region, *Seism. Res. Lett.* 68, 74-85.
- Anderson, J.G., (2002) Strong Motion Seismology, *Handbook of Earthquake and Engineering Seismology*, Chapter 57.
- Beresnev, I. A., Atkinson, G. M., (1997). Modeling Finite-fault radiation from the  $\omega^n$  spectrum. *Bull. Seism. Soc. Am.* 87(1), 67-84.
- Building and Housing Research Center, Tehran, Iran (<http://www.bhrc.ir>).
- Boore, D.M., (1983). Stochastic simulation of high-frequency ground motions based on seismological models of the radiated spectra. *Bull. Seism. Soc. Am.*, 73:1865–1894.
- Boore, D.M., Atkinson, G. (1987). Stochastic prediction of ground motion and spectral response parameters at hard-rock sites in eastern North America. *Bull. Seism. Soc. Am.*, 73, 1865-1894.
- D.M. Boore, "Simulation of ground motion using the stochastic method", *Pure Appl. Geophys.* 160, 635–676, 2003.
- Brune, J.N., (1970). Tectonic stress and the spectra of seismic shear waves from earthquakes", *J. Geophys. Res.*, 75, 4997-5010.
- Burridge, R., Willis, J. R., (1969). The self-similar problem of the expanding crack in an anisotropic solid", *Proc. Cambridge Phil. Soc.* 66, 443-468.
- Frankel, A., Thenhaus, P., Perkins, D., Leyendecker, E. V., (1995). Ground motion mapping- past, present and future", *Applied Technology Council publication ATC-35-1*, 7.1-7.40.
- Hartzell, S., (1978). Earthquake Aftershocks as Green's Functions, *Geophys. Res. Letters*, 5, 1-4.
- Hutchings, L., (1988). Modeling strong earthquake ground motion within earthquake simulation program EMPSYN that utilizes empirical Green's functions. UCRL-ID-105890, Lawrence Livermore National Laboratory, Livermore, California, 122.
- Hutchings, L., Wu, F., (1990). Empirical Green's functions from small earthquakes A waveform study of locally recorded aftershocks of the San Fernando earthquake. *J. Geophys. Res.*, 95, 1187-1214.
- Hutchings, L., (1991). Prediction of strong ground motion for the 1989 Loma Prieta earthquake using empirical Green's functions. *Bull. Seism. Soc. Am.* 81, 88-121.
- Hutchings, L., (1994). Kinematic earthquake models and synthesized ground motion using empirical Green's functions", *Bull. seism. Soc. Am.*, 84, 1028–50.
- Hutchings, L., Jarpe, S.P., Kasameyer, P.W., & Foxall, (1996). W., Synthetic strong ground motions for engineering design utilizing empirical Green's functions. *Proc. Fourth Caltrans Seismic Research Workshop*, p. 24; also presented at Eleventh World Conference of Earthquake Engineering, Acapulco, June 23–28, 1996 (CDROM Elsevier); available from Lawrence Livermore National Laboratory, Livermore, CA, UCRL-JC-123762.
- Hutchings, L., Ioannidou, E., Jarpe, S. & Stavrakakis, G.N., (1997). Strong Ground Motion Synthesis for a M=7.2 Earthquake in the Gulf of Corinth, Greece Using Empirical Green's Functions", Lawrence Livermore National Laboratory, Livermore, CA, UCRL-JC-129394.
- Hutchings, L., Ioannidou, E., Foxall, W., Voulgaris, N., (2007). A physically based strong ground-motion prediction methodology; application to PSHA and the 1999 Mw = 6.0 Athens earthquake. *Geophys. J. Int.* 168, 659–680.

- Irikura, K., Kamae, K., (1994). Estimation of strong ground motion in broad-frequency band based on a seismic source scaling model and an empirical Green's function technique. *Ann. Geophys.* 37, 1721–1743.
- Irikura, K., (1983). Semi-empirical estimation of strong ground motions during large earthquakes. *Bull. Disaster Res Inst.*, 33, 63-104.
- IYengar, R.N., Raghu Kanth, S.T.G., (2006). Strong Ground Motion Estimation during the Kutch, India Earthquake”, *Pure appl. geophys.* Vol.163, 153–173.
- Joyner, W.B., Boore, D.M., (1986). On simulating large earthquakes by Green's-function addition of smaller earthquakes, *Earthquake Source Mechanics. American Geophysical Monograph* 37, 6, 269-74.
- Kanamori, H., Anderson, D.L., (1975). Theoretical basis of some empirical relations in seismology. *Bull. Seism. Soc. Am.* 65(5), 1073-1095.
- Mori, J., (2001). Slip distribution of mainshock. In *A Comprehensive Survey of the 26 January 2001 Earthquake (Mw 7.7) in the State of Gujarat, India. Research Report on Natural Disasters*, Japan Ministry of Education, 41–45.
- NEHRP Recommended Provisions for Seismic Regulations for new Buildings and other Structures, 2000 Edition, and Prepared by the Building Seismic Safety Council for the Federal Emergency Management Agency, Washington D.C.
- Lam, N., Wilson, J., Hutchinson, G., (2000). Generation of Synthetic Earthquake Accelerograms Using Seismological Modelling: A Review. *Journal of Earthquake Engineering*, Vol. 4, No. 3, 321-354.
- Pitarka A., et al., (2000). Simulation of near-fault strong ground motion using hybrid Green's function, *Bull. Seismol. Soc. Am.* 90(3), 566–586.
- Poiata, N., Miyake, H., (2006). Broadband ground motion simulation of Romanian earthquakes using empirical green's function method. 13th ECEE & 30th General Assembly of the ESC, 506.
- Tumarkin, A.G., Archuleta, R.J., Madariaga, R., (1994). Basic scaling relations for composite earthquake models”, *Bull. Seism. Soc. Am.* 84, no. 4.
- Wennerberg, L., (1990). Stochastic summation of empirical Green's functions. *Bull. Seism. Soc. Am.* 80, 1418-1432.
- Wells, D.L., Coppersmith, K.L., (1994). New empirical relationships among magnitude, rupture width, rupture area, and surface displacement. *Bull. Seism. Soc. Am.*, 84: 974-1002.
- Wu, F.T., (1978). Prediction of strong ground motion using small earthquakes. 2nd International Microzonation Conference, San Francisco, 2,701-704.